

Omer Sinan Sahin
Emre Kahramanoglu
Ferdi Cakici
Emre Pesman



<http://dx.doi.org/10.21278/brod74101>

ISSN 0007-215X
eISSN 1845-5859

Control of dynamic trim for planing vessels with interceptors in terms of comfort and minimum drag

UDC 629.5.015.2:629.5.022.1:629.5.062.24

Original scientific paper

Summary

Nowadays, interceptors are often used to decrease total resistance and enhance comfort by reducing dynamic trim for high-speed planing vessels. They can be controlled manually as well as automatically by using a suitable closed-loop control system. Thus, in the present study, an automatically controllable system is presented to minimize the total resistance by reducing the dynamic trim in calm water. To reach this aim, a mathematical model which can represent the 2 degree of freedom vertical motion of a prismatic planing vessel is presented. The coefficients used in the model are calculated by using the Savitsky method. The standard dynamic trim angle and the optimum ones in terms of resistance are calculated by using the same method. For control action, a linear full state feedback control strategy (linear quadratic regulator) is applied, and instantaneous blade heights are found considering the change in forward speed. Therefore, the control-oriented model is able to change the blade height to reach the optimum trim angle in terms of the total resistance of the vessel for different forward speeds and speed profiles. The results show that the designed linear quadratic regulator control strategy is successful for reference trim tracking problems.

Key words: Planing hulls; interceptor; LQR; optimum trim

1. Introduction

With the technological developments in fast vessels, the need for them to be faster and more comfortable has emerged. While the speed of the vessel is increasing, comfort and security are expected to increase and fuel consumption is expected to decrease uncompromisingly. To overcome this challenge, an automatic control policy generally uses active actuators such as flaps and interceptors to follow a pre-calculated 'the best' dynamic trim angle for minimum drag. In order to obtain an efficient solution for this aim, the controller must be well-designed and sensitive [1].

Understanding of the dynamics of planing vessels began in 1964 with Daniel Savitsky. Savitsky [2] presented semi-empirical formulas for buoyancy, drag force, and center of pressure for a prismatic hull in calm water. When a planing hull reaches high speed, the

hydrodynamic buoyancy force becomes dominant, the displacement volume decreases, and the vessel starts to be planing regime on the water surface. Due to the reduced wetted area, a planing hull can reach higher speeds than a displacement-type hull [3]. Most of the planing vessel weight is supported by the hydrodynamic lift at high speed and the center of pressure shifts towards the bow of the vessel. Therefore they cause excessive trim and poor seakeeping performance. In addition to these hydrodynamic problems, these facts can cause poor comfort. However, appendages such as interceptor, trim tab, and transom wedge can be adopted to improve not only the seakeeping performance but also the comfort [4] while the optimization of conventional type of yachts can be made by changing the bulbous form [5],[6].

The appendages used to improve seakeeping and comfort for planing hulls can be active or passive for calm water as well as in waves [7]. However, the studies about these mechanisms showed that the change of the appendage configuration such as blade height, angle of attack, etc. can be more efficient not only in waves but also in calm water [8], [9], [10], [11]. In other words, introducing well-designed automatic control that drives the actuators actively is more useful compared to passive ones. However, to control them actively a mathematical model for actuators is needed.

The mathematical model of trim tab systems is generally based on Dawson and Blount method [12] and Brown formulas [13]. In these studies, it was stated how the additional hydrodynamic lift force created by the trim tab system is calculated. With the help of the equations presented in these studies, a mathematical relationship can be established between the trim tab and the interceptor. After almost 4 decades, Villa and Brizzolara [14] compared the hydrodynamic properties and performance of trim tabs and interceptors with computational fluid dynamics (CFD) simulations for dynamic trim of planing hulls. From the results obtained, they defined an equation between the flap angle of the trim tab and the blade height of the interceptor. After Dawson and Blount formulas, a new formula that defines the relationship between the flap angle of deflection and the equivalent interceptor of attack angle has been obtained from numerical results.

Since the trim tabs create an extra protrusion behind the vessel and cannot be closed completely, they can increase the friction force. To solve such negative effects, the interceptors used today have been developed. The main difference between the interceptors and trim tabs is the deflection angle from the keel of the hull. The difference in deflection angle will result in smaller surface areas of the interceptors in contact with water compared to the trim tabs, and the resulting increase in resistance will be less. The interceptor systems generally consist of two active flaps, which are located on the port and starboard side perpendicular to the stern of the boat. These flaps, which move linearly, can be controlled automatically. In addition, the flaps can work simultaneously and independently of each other. The flaps create additional lifting pressure beneath the boat, and in the case of controllable interceptors, the plate can be extended or retracted as needed to increase or reduce the amount of lift.

In the literature, there are experimental and numerical studies conducted to understand the effects of the interceptor system on planing hulls. Savitsky [15] mentioned that an active control system that can be located on the transom of the boat can be useful to reduce motions and accelerations. In his study, he examined the effect of controllable flaps on heave and pitch. Towing tank test results showed that heave motion could be damped by 50% and pitch motion by 70%. Tsai and Hwang [16] conducted model tests to determine the effect of a stern flap, interceptor, and integrated interceptor with stern flap on the resistance performance of a high-speed planing vessel. Test results showed that the resistance reduction effect is greatest between Froude number (Fr) 2.0-2.5. Xi and Sun [17] developed a nonlinear controller to reduce the porpoising instability of high-speed planing vessels using controllable transom

flaps. The controller was designed based on feedback linearization, and the controller's performance was verified in the simulation. Rijkens et al. [18] conducted vertical motion modeling based on the model test data and controlled the vertical motion using a stern flap and an interceptor. The controller was designed using Proportional-Integral-Derivative (PID) control, and the controller performance was validated through simulation. Ghassemi et al. [19] investigated under which conditions a planing hull can provide its optimum performance at different speeds. In addition, it was shown that the appropriate interceptor blade height varies according to the Froude number. Day and Cooper [20] studied the effect of interceptors on the drag reduction of high-performance sailing yachts. The interceptor exhibited a 10–18% resistance reduction over the speed range of 8–20 knots, and the resistance reduction was larger than trim changes by moving ballast longitudinally. Seo et al. [21] presented the application of devices such as trim tabs, interceptors, transom wedges, and integrated transom wedges-tabs to control the dynamic trim and improvement of fuel efficiency of the vessel. The model test results showed that the optimum appendage was the interceptors and they produced 5% fuel saving and 1.2 degrees of trim reduction in design speed. In addition to this, the results showed that the reduction of resistance can reach 7% at the maximum speed. Karimi et al. [22] demonstrated that the heave, pitch motion, and vertical accelerations can be reduced by an interceptor through model tests on the performance of high-speed catamaran planing boats in calm water and waves. They designed a vertical motion controller for planing boats using a linear quadratic regulator (LQR) feedback controller. In the simulation, it was confirmed that the pitch motion of the vessel is reduced by active control in head sea conditions. The application of a controlled stern interceptor results in pitch and heave reductions were up to 25% and 20%. Mansoori et al. [10] presented a numerical study to provide a convenient method for determining interceptor dimensions. They stated that the height of the interceptor should be between 0.1 and 0.6 times the boundary layer thickness at the stern of the planing boat. Sakaki et al. [23] evaluated the hydrodynamic performance of a boat with a trim tab and interceptor attachment using a genetic algorithm (GA). In their study, they generated planing boats with a trim tab and an interceptor by using Savitsky's equations with GA. Optimization by changing the deadrise angle showed that the total resistance decreased at different deadrise angles. Park et al. [4] showed that the interceptor effect can be improved not only in still water but also in regular and irregular waves with a controllable blade height mechanism, thus reducing both vertical motions and fuel consumption. As a result of their study, the pitch motion was reduced by up to 41.3% in the regular wave and 32.4% in the irregular wave by a controllable interceptor system.

In the present paper, the LQR controller is designed for tracking the optimum trim angle of the planing vessel in calm water for minimum drag by using a highly nonlinear mathematical model. In order to obtain a linear state space model for the LQR design, the system is linearized around the zero motion equilibrium point. When the current literature is surveyed, to the best knowledge of the authors no such work addresses the reference tracking problem by using transom interceptors for this kind of fast vessel. Therefore, the main purpose of the study is to calculate the required interceptor blade heights for minimum drag at different vessel velocities and velocity profiles as well. The present paper is organized as follows: Section 2 describes the mathematical model of the planing vessel in calm water. The LQR strategy is presented in Section 3. Section 4 gives the simulation results of the LQR for different velocity profiles of the vessel in calm water. Section 5 gives conclusion remarks about the study. The paper is further structured into subsections for better readability.

2. Mathematical Model

In this section, a mathematical model for planing vessels with controllable interceptors is presented. The presented model ensures tools for understanding high-speed vessel physics and control design.

2.1 The Coordinate System and the Hull with Interceptor

A right-handed coordinate system is chosen for the mathematical model. The chosen coordinate system is described for the planing vessel in Figure 1.

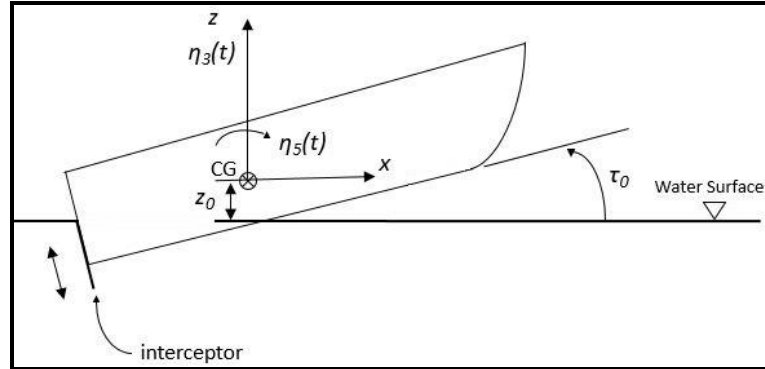


Fig. 1 The coordinate system of the prismatic planing vessel

The trim angle is defined as τ_0 at the running attitude. The vertical distance of the center of gravity (COG) from the water surface is also defined as z_0 . η_3 and η_5 depict the heave and pitch motions, respectively. The pitch motion means the rotation of the vessel relative to the defined inertial frame that is fixed at the center of gravity. It should be mentioned that η_3 and η_5 are positive upward and bow down.

In the present study, a monohedral (prismatic) hull form with a constant deadrise angle is used in all analyses. Within the scope of the TUBITAK Teydeb-1507 project (Project Number: 7190739), the authors have already produced an interceptor mechanism that can be suitable for the 4-10 m planing hulls. The main particulars of the vessel used in this study are listed in Table 1 where L, B, LCG and VCG represent the length overall, beam, longitudinal center of gravity and vertical center of gravity respectively. Figure 2 shows the 2D and 3D views of the hull form which was re-scaled from the original form produced by Begovic and Bertorello [24]. Please note that the selected planing hull form can be assumed as a benchmark because several investigations have been carried out by using this form [9].

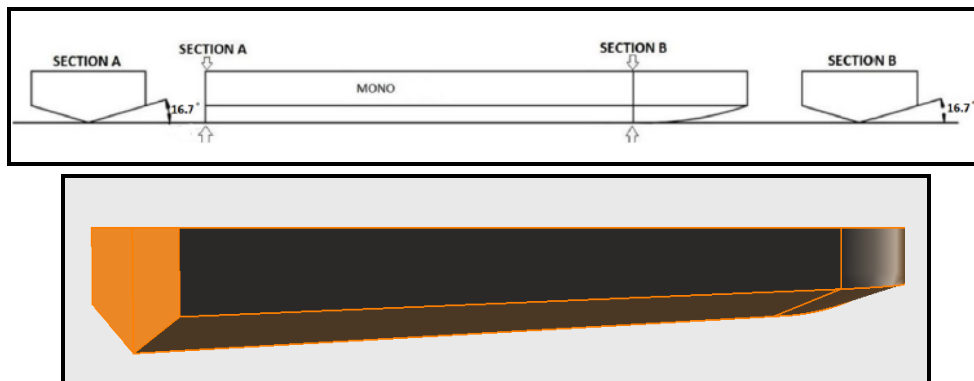


Fig. 2 2D-3D view of the monohedral hull form [22]

Table 1 Main particulars of the vessel used in the present study

Feature	Value	Unit
L	4.750	m
L / B	4.481	-
T / B	0.226	-
Static Trim	1.660	deg
$\Delta / (\rho g B^3)$	0.428	-
kyy / B	1.375	-
β	16.70	deg
LCG / L	0.369	-
VCG / L (from the keel)	0.075	-

Table 2 Main particulars of the interceptor

Feature	Value	Unit
Span / B	0.2830	-
Maximum height (h_{max}) / B	0.0472	-
Thickness / B	0.0057	-

The twin interceptor configuration is located in the stern and the main particulars of the interceptor are listed in Table 2. The closed configuration (off) and the maximum height condition (fully on) are shown in Figure 3. It should be noted that blade height (h) may vary between 0 and 50 mm ($h/B = 0.0472$). Figure 4 shows the interceptor layout measurements.

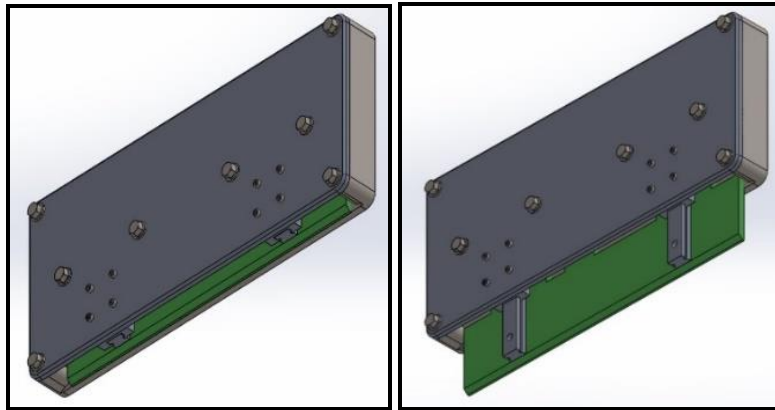


Fig. 3 Interceptor is off (left) and on (right)

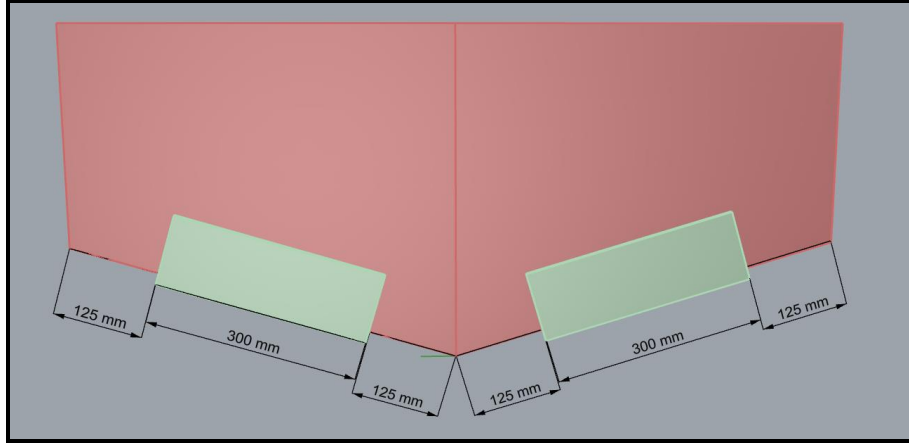


Fig. 4 The layout of the interceptor

2.2 Equations of Motion

The Equations of the motion for heave and pitch motions are described following the expressions presented in Troesch [25]. Equation (1) represents the heave motion while Equation (2) represents the pitch motion where $\tau(t)$ and $z(t)$ are the effective trim angle of the vessel and the effective vertical distance of the COG of the vessel from the calm water surface.

$$\eta_3(t) = z(t) - z_0 \quad (1)$$

$$\eta_5(t) = -\tau(t) + \tau_0 \quad (2)$$

On the other hand, τ_0 and z_0 denote the trim angle and vertical distance of the COG of the vessel from the calm water surface at running attitude. The presented mathematical model contains heave and pitch motions and it is assumed to be decoupled with surge motion for small trim angles. Therefore, the motion equation of the planing vessel with controllable actuators operating in the calm water can be written as follows:

$$\bar{M}\dot{\eta} + D\dot{\eta} = F^R + F^{FL} \quad (3)$$

where

$$\eta = \begin{bmatrix} \eta_3 \\ \eta_5 \end{bmatrix}, F^R = \begin{bmatrix} F_3^R \\ F_5^R \end{bmatrix}, F^{FL} = \begin{bmatrix} F_3^{FL} \\ F_5^{FL} \end{bmatrix}$$

$$\bar{M} = \begin{bmatrix} M + A_{33} & A_{35} \\ A_{53} & I_y + A_{55} \end{bmatrix}, D = \begin{bmatrix} B_{33} & B_{35} \\ B_{53} & B_{55} \end{bmatrix}$$

Here, the dot product denotes the derivative with respect to time. M denotes the mass of the vessel while I_y denotes the pitch moment of inertia about COG. A_{ij} and B_{ij} are the radiation coefficients (the added mass and damping) although i and j can be 3 or 5 in accordance with the motion. F_3^R and F_5^R are the heave and pitch restoring forces, respectively. It is noted that F_3^{FL} and F_5^{FL} are the flap forces in heave and pitch directions,

respectively and they will be changed to interceptor blade heights using the method offered by Dawson and Blount [12], please see section 2.5.

2.3 Radiation Coefficients

For added mass and damping coefficients, the experimental study of Troesch [25] is used and the change of the values with respect to the wave frequency is ignored since the paper is interested in calm water operations. Although the added mass and damping values are the non-linear functions of the motion amplitude, this nonlinearity is still small compared to restoring terms and it is neglected. Therefore A and B matrices are assumed to be constant matrices at a given vessel speed. Their values are calculated using the experimental data with a first-order polynomial fit depending upon the forward speed of the vessel. Please see Section 2.6 for details.

2.4 Restoring Terms

With the consideration of a simpler version of restoring forces recommended by Savitsky [2], F_3^R and F_5^R can be calculated as follows:

$$F_3^R(t) = N(t) \cos(\tau_0 - \eta_5(t)) - Mg \quad (4)$$

$$F_5^R(t) = -N(t) \cos(l_p(t) - LCG) \quad (5)$$

Savitsky [2] presented empirical formulations to compute the restoring forces as functions of the mean wetted aspect ratio which is defined as $\lambda(t)$ and the effective trim angle which is defined as $\tau(t)$. The related expressions are given as follows:

$$C_{L0}(t) = \tau(t)^{1.1} \left(0.012\lambda(t)^{0.5} + \frac{0.0055\lambda(t)^{2.5}}{Fr_B^2} \right) \quad (6)$$

$$C_{L\beta}(t) = C_{L0}(t) - 0.0065\beta C_{L0}(t)^{0.6} \quad (7)$$

$$N(t) = 0.5\rho V^2 B^2 C_{L\beta}(t) (\cos \tau(t)) \quad (8)$$

$$l_p(t) = \lambda(t) B \left(0.75 - \frac{1}{5.21 \left(\frac{Fr_B}{\lambda(t)} \right)^2 + 2.39} \right) \quad (9)$$

Where Fr_B (-) denotes the beam Froude number and V (m/s) denotes the forward speed. B (m) denotes the vessel beam, C_{L0} (-) denotes the lift coefficient for a zero deadrise flat surface, $C_{L\beta}$ (-) denotes the lift coefficient for the surface with a constant deadrise angle of β (deg), ρ (kg/m^3) denotes the water density, g (m/s^2) denotes the gravity constant. $\lambda(t)$ can be calculated as follows where VCG denotes the vertical distance of COG from the keel, and LCG denotes the longitudinal distance of COG from the transom.

$$\lambda(t) = \frac{1}{B} \left[LCG + \frac{VCG}{\tan(\tau_0 - \eta_5(t))} - \frac{(z_0 + \eta_3(t))}{\sin(\tau_0 - \eta_5(t))} \right] \quad (10)$$

2.5 Forces Induced by Interceptor

Forces created by interceptors can be determined using the equivalent flap angle formulation presented by Dawson and Blount [12]. In this experimental data-based approach, it is assumed that the flap and the interceptor have the same width and the maximum flap angle is taken as 15 degrees. The geometric interpretation of the approach is shown in Figure 5.

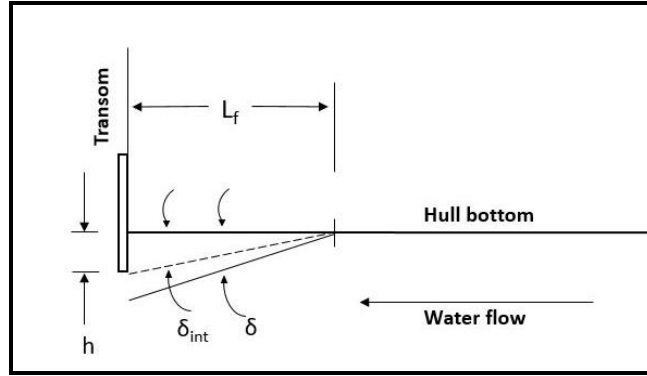


Fig. 5 The logic for the transition from the flap to the interceptor [9]

As known well, Savitsky and Brown [26] provided empirical formulations to calculate the forces based on the transom flaps. The flap lift F_3^F and the flap moment F_5^F about COG can be found as follows:

$$F_3^F = 0.023L_F\sigma B\rho V^2\delta \quad (11)$$

$$F_5^F = (0.023L_F\sigma B\rho V^2)(0.6B + L_F(1-\sigma))\delta \quad (12)$$

Where L_F (m) denotes the equivalent flap chord length. σ (-) denotes the flap span-beam ratio. δ (deg) flap angle. According to the experimental work of Dawson and Blount [10], δ (deg) flap angle can be expressed with an equivalent geometric angle for interceptor δ_{int} (deg), under the restriction of maximum flap angle as 15 degrees, defined in Equation (13). The interceptor blade height (h) can be calculated as defined in Equation (14).

$$\delta_{int} = 0.175\delta + 0.0154\delta^2 \quad (13)$$

$$h = L_F \sin(\delta_{int}) \quad (14)$$

A virtual flap was considered and L_F is taken $0.25B$. In addition, $\sigma=1$ was taken by assuming the flap span is equivalent to the beam. These values were chosen by considering the present hull dimensions and benefiting the current literature [17], [26].

2.6 Linearized Mathematical Model

To design an LQR controller, the mathematical model should be linearized. The linearized model is given with Equation (15).

$$\bar{M}\ddot{\eta} + D\dot{\eta} + R\eta = \chi\delta \quad (15)$$

The reason for the nonlinearity in Equation (3) is the restoring terms and these terms can be linearized around the zero heave and pitch motions as follows where i and j are equal to 3 or 5.

$$R_{ij} = -\frac{\partial F_i}{\partial \eta_j} \quad (16)$$

around $\eta_j = 0$ and where

$$\eta = \begin{bmatrix} \eta_3 \\ \eta_5 \end{bmatrix}, \chi = \begin{bmatrix} 0.023L_F\sigma B\rho V^2 \\ (0.023L_F\sigma B\rho V^2)(0.6B + L_F(1-\sigma)) \end{bmatrix},$$

$$\bar{M} = \begin{bmatrix} M + A_{33} & A_{35} \\ A_{53} & I_y + A_{55} \end{bmatrix}, D = \begin{bmatrix} B_{33} & B_{35} \\ B_{53} & B_{55} \end{bmatrix}, R = \begin{bmatrix} C_{33} & C_{35} \\ C_{53} & C_{55} \end{bmatrix}$$

According to data supplied from Troesch [25] and using first-order curve fitting, added mass and damping coefficients in the \bar{M} and D matrices are obtained by a function of Fr_B (C_V) as follows:

$$\left. \begin{aligned} A_{33} &= (1.118C_V - 1.2292)\rho B^3 \\ B_{33} &= (0.3685C_V + 1.4362)\rho B^3\sqrt{g/B} \\ A_{53} &= (0.4191C_V - 0.457)\rho B^4 \\ B_{53} &= (-1.3765C_V + 1.2538)\rho B^4\sqrt{g/B} \\ A_{55} &= (0.0609C_V + 1.4384)\rho B^5 \\ B_{55} &= (1.839C_V + 0.3002)\rho B^5\sqrt{g/B} \\ A_{35} &= (-0.4348C_V + 1.2448)\rho B^4; \\ B_{35} &= (2.3701C_V - 1.9203)\rho B^4\sqrt{g/B} \end{aligned} \right\} \quad (17)$$

After calculating the flap angle, the corresponding interceptor blade height can be determined by using Equation (13) and Equation (14). To perform the derivation in Equation (16), Equation (4) and Equation (5) are calculated for relatively small heave and pitch motions, and obtained values are plotted as in Figure 6. After the implementation, the second-order polynomial fit, C_{33} , C_{53} , C_{35} and C_{55} are found as -43388, 42496, 4973 and -83842.

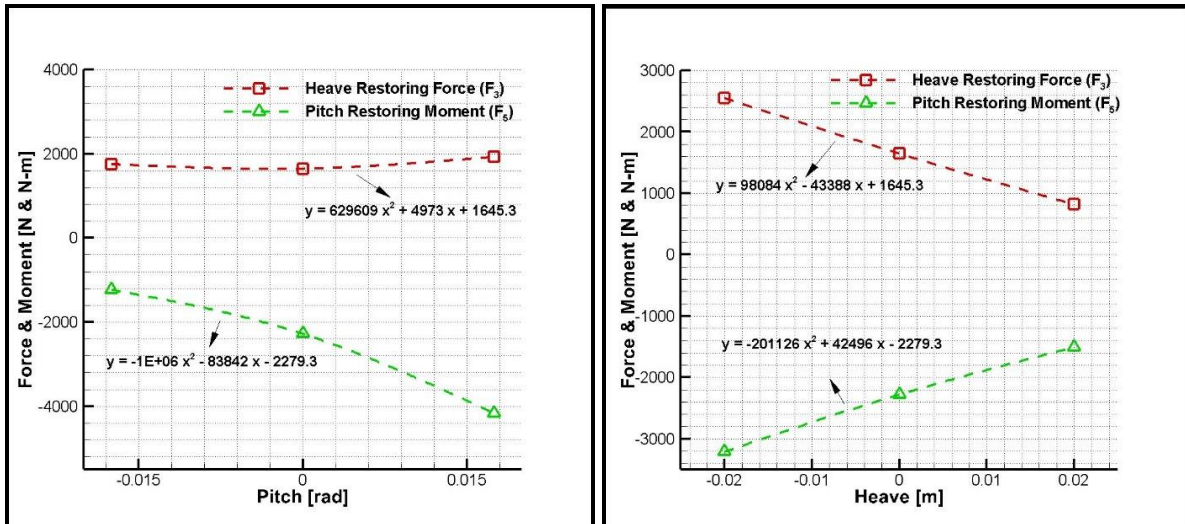


Fig. 6 The linearization process for the restoring terms

3. Control Design

Although the mathematical model is complex, the first attempt for controller design is to design an LQR. For this purpose, the linearized model given in Section 2.6 is used. To have a constant system matrix, added mass and damping coefficients are calculated at $Fr_B=2$. The state-space model is used as a control-oriented model as follows:

$$\frac{d}{dt}x(t) = Ax(t) + B[\delta(t)] \quad (18)$$

$$\text{where } x(t) = \begin{bmatrix} \eta_3 \\ \eta_5 \\ \dot{\eta}_3 \\ \dot{\eta}_5 \end{bmatrix},$$

$$A = \begin{bmatrix} \text{zeros}(2) & \text{eye}(2) \\ -\bar{M}^{-1}R & -\bar{M}^{-1}D \end{bmatrix}, \quad B = \begin{bmatrix} \text{zeros}(2,1) \\ 0.023L_F\sigma B\rho V^2 \\ \bar{M}^{-1} \left[(0.023L_F\sigma B\rho V^2)(0.6B + L_F(1-\sigma)) \right] \end{bmatrix}$$

$\delta(t)$ is the control input representing flap angle in Equation (18) and it will be transformed to interceptor blade height. For the reference track problem, an error vector between measured pitch angle and reference pitch angle is defined as $\dot{e}(t) = \eta_5 - \eta_{5REF}$ where η_5 is instantaneous pitch motion and η_{5REF} is the optimum effective trim angle calculated using the Savitsky method as a function of vessel Fr_B . Systematic Savitsky analysis is performed to obtain the minimum drag conditions at different Fr_B by manipulating the dynamic trim angle of the hull with an energy-saving device such as flaps and interceptors. Detailed information on the calculation of optimum trim angles for minimum drag can be found in the work of Sancak and Cakici [27].

If the state space equations are rearranged considering the added error vector, the augmented state-space system is obtained as follows:

$$\frac{d}{dt}x_{new}(t) = A_{new}x_{new}(t) + B_{new}[\delta(t)] + B_2\eta_{5REF}(t) \quad (19)$$

where

$$x_{new}(t) = \begin{bmatrix} \eta_3 \\ \eta_5 \\ \dot{\eta}_3 \\ \dot{\eta}_5 \\ \dot{e} \end{bmatrix}, \quad A_{new} = \begin{bmatrix} A & \text{zeros}(4,1) \\ 0 & 1 & 0 & 0 & 0 \end{bmatrix}, \quad B_{new} = \begin{bmatrix} B \\ 0 \end{bmatrix}, \quad B_2 = \begin{bmatrix} 0 \\ 0 \\ 0 \\ 0 \\ -1 \end{bmatrix}$$

For minimization of $\dot{e}(t)$, the designed controller will minimize the quadratic cost function given in Equation (20) by the use of the state variables and control actions.

$$J = \int_0^{\infty} [\mathbf{x}_{new}^T(t) \mathbf{Q} \mathbf{x}_{new}(t) + \delta(t)^T \mathbf{R} \delta(t)] dt \quad (20)$$

The solution of Equation (20) gives the well-known Ricatti Equation as follows:

$$\mathbf{A}_{new}^T \mathbf{P} + \mathbf{P} \mathbf{A}_{new} - \mathbf{P} \mathbf{B}_{new} \mathbf{R}^{-1} \mathbf{B}_{new}^T \mathbf{P} + \mathbf{Q} = 0 \quad (21)$$

$$\delta(t) = \mathbf{K} \mathbf{x}_{new}(t) \quad (22)$$

$$\mathbf{K} = -\mathbf{R}^{-1} \mathbf{B}_{new}^T \mathbf{P} \quad (23)$$

where \mathbf{R} and \mathbf{Q} are weighting matrices and they are selected as follows:

$$\mathbf{Q} = \begin{bmatrix} 1 & 0 & 0 & 0 & 0 \\ 0 & 10 & 0 & 0 & 0 \\ 0 & 0 & 1 & 0 & 0 \\ 0 & 0 & 0 & 1 & 0 \\ 0 & 0 & 0 & 0 & 1 \end{bmatrix}, \quad \mathbf{R} = [1e-6] \quad (24)$$

\mathbf{K} is calculated as given below and finally obtained flap angles δ are transformed into interceptor blade height h by using Equation (13) and Equation (14).

Since matrices \mathbf{A} and \mathbf{B} are dependent on the vessel velocity V , the control law matrix \mathbf{K} should be calculated in the loop as the velocity of the vessel changes. However, the close loop simulation results showed that taking the \mathbf{K} matrix as time-invariant gives more stable results than that of the time-varying \mathbf{K} matrix. Therefore, \mathbf{K} is calculated for a medium Fr_B ($Fr_B=2$) and found as follows:

$$\mathbf{K} = 10^3 [2.5045 \quad 0.5941 \quad 0.8623 \quad 0.7524 \quad 1.000] \quad (25)$$

4. Simulation Results

To obtain simulation results, the standard and optimum trim angles in terms of minimum drag should be known prior. For this, the Savitsky method is employed and the standard and optimum dynamic trim angles are obtained for each Fr_B . Please see the work of Sancak and Cakici [27] for more details. Then a second-order polynomial is fitted to capture the normal and optimum trim angles of the vessel concerning vessel operations speed. For this aim, three different typical forward velocity profiles that range the operational speed of this kind of vessel are predefined as seen in Figure 7. On the figure captions, VP means the velocity profile with respect to time. It is noted that the difference only comes from the periods that the velocity of the vessel is kept to a constant velocity. It is interesting to note that the defined velocity range is taken between $Fr_B=1.50$ and $Fr_B=2.50$ which are typical speed ranges for interceptor usage [9].

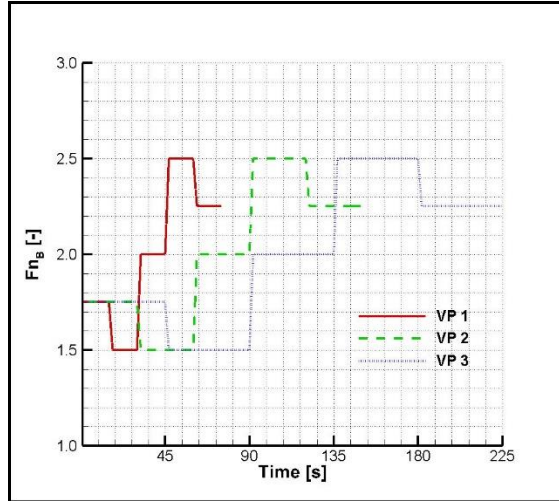


Fig. 7 The pre-defined velocity profiles (VP)

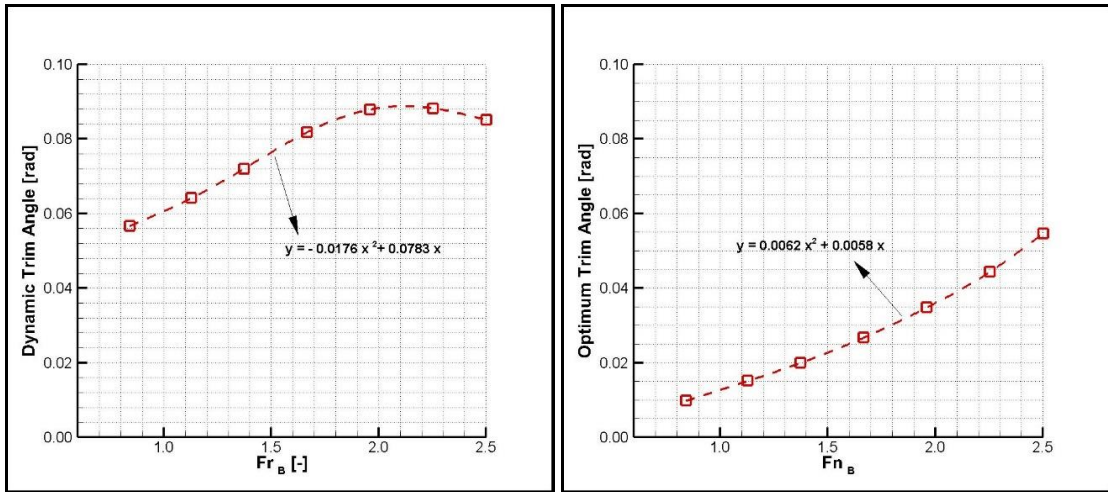


Fig. 8 The dynamic trim angles (left) and the optimum ones (right) in terms of minimum drag for different velocities

Figure 8 is given for the standard and optimum trim angles of the subjected planing vessel by using the methodology presented in Sancak and Cakici [27]. The calculated LQR control law is used in the nonlinear model, and the results are given in Figures 9 to 11. In these figures, while the optimum trim signal induced by interceptor is obtained by the difference of dynamic trim angle and the optimum trim angle that is found using a second-order polynomial given in Figure 8 (right), the trim (LQR) signal is obtained with the control action of the interceptor blade. Figures 9 (right), 10 (right) and 11 (right) show the blade heights with respect to time for each velocity profile. Figure 9 represents the most aggressive velocity profile. In this case, the velocity of the vessel changes very rapidly and the responses of the interceptors are relatively slow compared to the other two cases. Almost from the beginning ($Fr_B=2$) to $t=45$ seconds, the LQR fails to track the optimum trim angle as seen in Figure 9 (left). The main reason for this failure is thought that more control effort is required to bring the very low initial trim angle (around 0 degrees) to a relatively higher optimum angle (around 3 degrees).

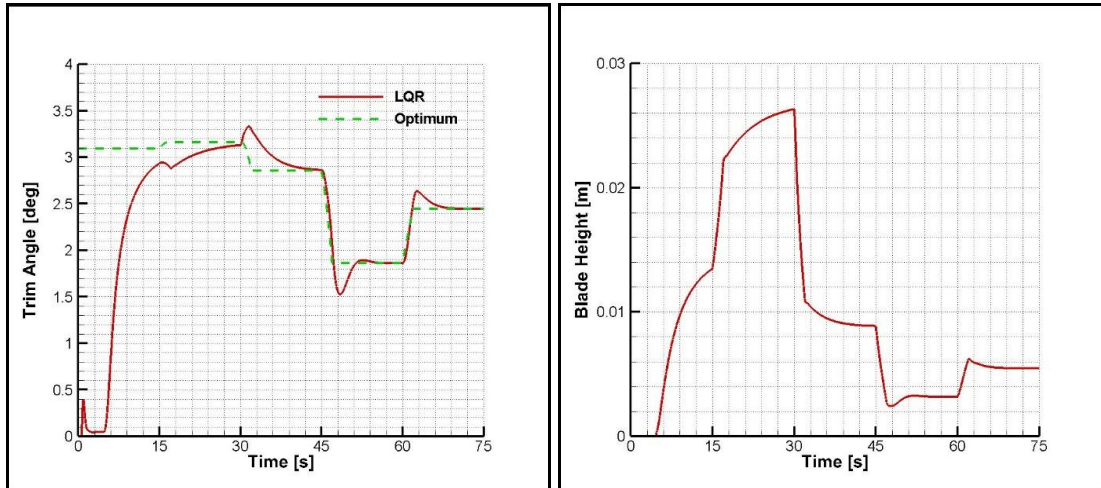


Fig. 9 The LQR controlled trim vs. optimum trim (left) and blade heights with respect to time for VP1

Figure 10 represents the second velocity profile (VP2) which is middle-level aggressive. The velocity changes are slow compared to VP1 but fast compare to VP3. In this case, LQR is quite successful to capture the optimum trim angles of the vessel. Only some reference tracing failure is depicted at the beginning of the operation that emerges from the low initial trim angle of the vessel as seen in Figure 10 (left).

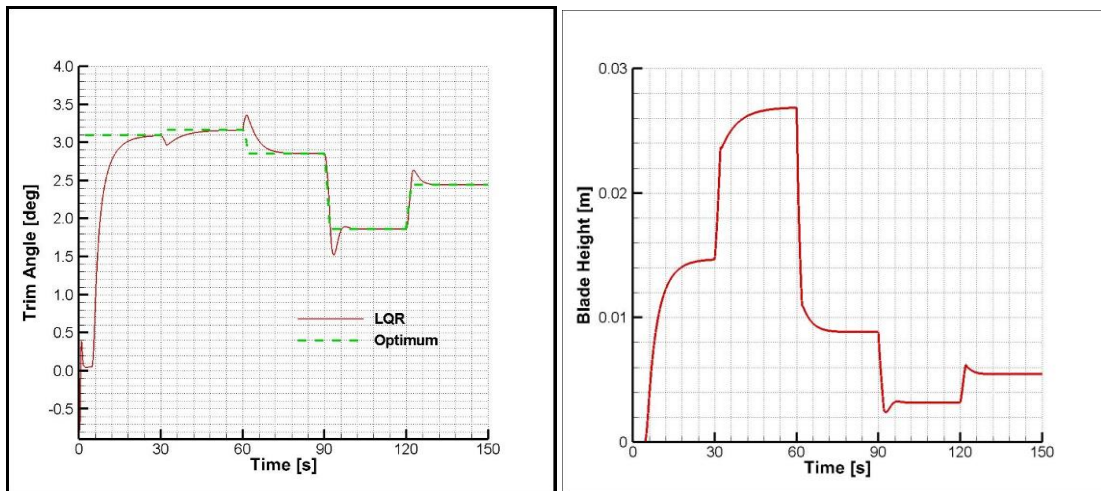


Fig. 10 The LQR controlled trim vs. optimum trim (left) and blade heights with respect to time for VP2

Figure 11 represents the third velocity profile (VP3) which is the mildest case out of defined scenarios and it is thought to be the most realistic one. In this case, LQR is very successful to capture the optimum trim angles of the vessel at varying velocities. It should be noted that, in all scenarios, the maximum interceptor blade height remains in the allowed range recommended by the study of Sahin et al. [9].

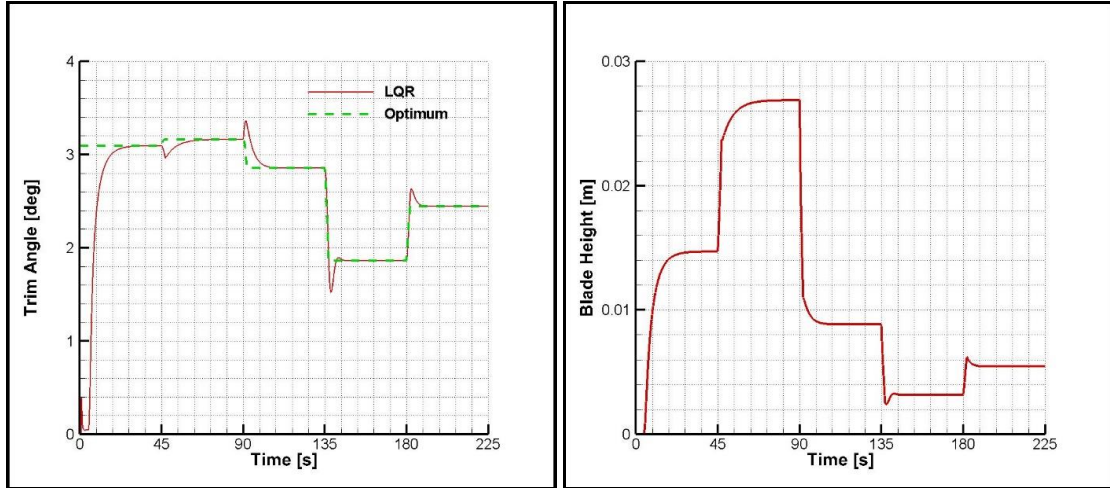


Fig. 11 The LQR controlled trim vs. optimum trim (left) and blade heights with respect to time for VP3

Table 3 illustrates the reached optimum interceptor blade heights obtained from the simulations and the optimum trim angles in terms of Fr_B .

Table 3. The optimum blade heights and trim angles

Fr_B [-]	Blade Height [mm]
1.50	26.86
1.75	14.68
2.00	8.824
2.25	5.458
2.50	3.176

5. Conclusion Remarks

In the present study, an LQR controller is designed to track the optimum trim angle for minimum drag by using a non-linear mathematical model of a planing hull. The radiation terms in the model are obtained using the data presented by Troesch [25] while the restoring terms in the model are calculated using the Savitsky formulas [2]. Similar to this, the optimum trim angles for the selected planing hull are obtained using the same semi-empirical method widely used in the literature. The optimum blade heights for different velocity profiles are obtained considering the optimum trim angles and then the controller changes the blade heights with respect to the change in velocity. The following outcomes are reported from the study:

- The interceptor blade height corresponding to the flap angle was determined using Equation (13) and Equation (14). It has been seen that it is possible to obtain the mathematical model of the interceptor by using the trim tab model.
- According to the command from the designed LQR controller, the interceptor blade height can be changed as required.
- In different velocity profiles, the LQR controller approach is tested and it is found that VP2 and VP3 velocity profiles are successfully tracked. Since the VP1 profile is rapidly changing, the LQR fails especially at beginning of the operation. Therefore,

the designed LQR controller is successful in the reference trim tracking problem for relatively slowly changing velocity profiles.

The authors comment that any uncertainty in the geometry of the model or the coefficients in the mathematical model should be compensated with the use of feedback logic. In future works, it is planned to investigate the effects of regular and random waves on the reference trim tracking problem. To overcome such disturbance effects, different control strategies will be developed.

Acknowledgements

The Scientific and Technological Research Council of Turkey (TUBITAK) supports this study within the scope of the Teydeb-1507 project (Project Number: 7190739).

REFERENCES

- [1] De la Cruz, J.M., Girson-Sierra, J., Aranda, J. and Esteban, S., 2004. Improving the Comfort of a Fast Ferry. *IEEE Control Systems*, 24(2), 47-60. <https://doi.org/10.1109/MCS.2004.1275431>
- [2] Savitsky, D., 1964. Hydrodynamic Design of Planing Hulls. *Marine Technology*, 1 (1), 71-99. <https://doi.org/10.5957/mt1.1964.1.4.71>
- [3] Lewis, E.V., 1988. Principles of naval architecture: Volume 2 Resistance, propulsion and vibration. *The Society of Naval Architects and Marine Engineers*, Jersey City, New Jersey.
- [4] Park, J.-Y., Choi, H., Lee, J., Choi, H., Woo, J., Kim, S., Kim, D.J., Kim, S.Y., Kim, N., 2019. An experimental study on vertical motion control of a high-speed planing vessel using a controllable interceptor in waves. *Ocean Engineering*, 173, 841–850. <https://doi.org/10.1016/j.oceaneng.2019.01.019>
- [5] Degiuli, N., Farkas, A., Martić, I., Zeman, I., 2021. Numerical and experimental assessment of the total resistance of a yacht. *Brodogradnja*, 72(3), 61-80, <https://doi.org/10.21278/brod72305>
- [6] Zhao, C., Wang, W., Jia P., Xie Y., 2021. Optimisation of hull form of ocean-going trawler. *Brodogradnja*, 72(4), 33-46, <https://doi.org/10.21278/brod72403>
- [7] Jangam, S., Sahoo, P., 2021. Numerical investigation of interceptor effect on seakeeping behaviour of planning hull advancing in regular head waves. *Brodogradnja*, 72(2), 73–92. <https://doi.org/10.21278/brod72205>
- [8] Avci, A.G., Barlas, B., 2018. An experimental investigation of interceptors for a high speed hull. *International Journal of Naval Architecture and Ocean Engineering*, 11(1), 256-273. <https://doi.org/10.1016/j.ijnaoe.2018.05.001>
- [9] Sahin, O.S., Kahramanoglu, E., Cakici, F., 2022. Numerical evaluation on the effects of interceptor layout and blade heights for a prismatic planing hull. *Applied Ocean Research*, 127(1), 103302. <https://doi.org/10.1016/j.apor.2022.103302>
- [10] Mansoori, M., Fernandes, A. C., Ghassemi, H., 2017. Interceptor design for optimum trim control and minimum resistance of planing boats. *Applied Ocean Research*, 69, 100–115. <https://doi.org/10.1016/j.apor.2017.10.006>
- [11] Samuel, S., Mursid, O., Yulianti, S., Kiryanto, Iqbal, M., 2022. Evaluation of interceptor design to reduce drag on planing hull. *Brodogradnja*, 73(3), 93-110. <https://doi.org/10.21278/brod73306>
- [12] Dawson, D. and Blount, D., 2002. Trim Control. *Professional Boatbuilder*, 140-149.
- [13] Brown, P. W., 1971. An Experimental and Theoretical Study of Planing Surfaces with Trim Flaps. *Stevens Institute of Technology*, Davidson Laboratory, Hoboken, New Jersey. <https://doi.org/10.21236/AD0722393>
- [14] Villa, D., Brizzolara, S., 2009. A systematic CFD analysis of flaps / interceptors hydrodynamic performance. *10th International Conference on Fast Sea Transportation*, Athens, Greece.
- [15] Savitsky, D., 2003. On the subject of high-speed monohulls. *Presented to the Greek Section of the Society of Naval Architects and Marine Engineers*, Athens, Greece.

- [16] Tsai, J.F., Hwang, J.L., 2004. Study on the compound effects of interceptor with stern flap for two fast monohulls. *Oceans'04. MTS/IEEE Techno-Ocean'04*, 2, 1023–1028.
- [17] Xi, H., Sun, J., 2006. Feedback stabilization of high-speed planing vessels by a controllable transom flap. *IEEE Journal of Ocean Engineering*, 31(2), 421–431. <https://doi.org/10.1109/JOE.2006.875097>
- [18] Rijkens, A.A.K., Keuning, J.A., Huijsmans, R.H.M., 2011. A computational tool for the design of ride control systems for fast planing vessels. *International Shipbuilding Progress*, 58(4), 165–190. <https://doi.org/10.3233/ISP-2012-0074>
- [19] Ghassemi, H. M., Mansouri, M., Zaferanlouei, S., 2011. Interceptor Hydrodynamic Analysis for Handling Trim Control Problems in the High-speed Crafts. *Journal of Mechanical Engineering Science*, 225, 2597–2618. <https://doi.org/10.1177/0954406211406650>
- [20] Day, A.H., Cooper, C., 2011. An experimental study of interceptors for drag reduction on high-performance sailing yachts. *Ocean Engineering*, 38(8), 983–994. <https://doi.org/10.1016/j.oceaneng.2011.03.006>
- [21] Seo, K. Gopakumar, N., Atlar, M., 2013. Experimental investigation of dynamic trim control devices in fast speed vessel. *Journal of Navigation and Port Research*, 37(2), 137–142. <https://doi.org/10.5394/KINPR.2013.37.2.137>
- [22] Karimi, M.H., Seif, M.S., Abbaspour, M., 2013. A study on vertical motions of high-speed planing boats with automatically controlled stern interceptors in calm water and head waves. *Ships and Offshore Structure*, 10, 335–348. <https://doi.org/10.1080/17445302.2013.867647>
- [23] Sakaki, A., Ghassemi, H., Keyvani, S., 2018. Evaluation of the Hydrodynamic Performance of Planing Boat with Trim Tab and Interceptor and Its Optimization Using Genetic Algorithm. *Journal of Marine Science and Application*, 18(2), 131–141. <https://doi.org/10.1007/s11804-018-0040-6>
- [24] Begovic, E., Bertorello, C., 2012. Resistance assessment of warped hullform. *Ocean Engineering*, 56, 28–42. <https://doi.org/10.1016/j.oceaneng.2012.08.004>
- [25] Troesch, A.W., 1992. On the Hydrodynamics of Vertically Oscillating Planing Hull. *Journal of Ship Research*, 36(4), 317–331. <https://doi.org/10.5957/jsr.1992.36.4.317>
- [26] Savitsky, D., Brown, P., 1976. Procedure of Hydrodynamic Evaluation of Planing Hull in Smooth and Rough Water. *Journal of Marine Technology*, 13, 381–400. <https://doi.org/10.5957/mtl.1976.13.4.381>
- [27] Sancak, E., Cakici, F., 2021. Determination of the Optimum Trim Angle of Planing Hulls for Minimum Drag Using Savitsky Method. *GMO Journal of Ship and Marine Technology*, 220, 43–53. <https://doi.org/10.54926/gdt.951371>

NOMENCLEATURE

A_{ij}	Added mass coefficients	LQR	Linear Quadratic Regulator
B_{ij}	Damping coefficients	M	Mass
B	Beam	\bar{M}	Mass matrix
C_{ij}	Restoring coefficients	T	Draught
C_{L0}	Lift Coefficient for zero deadrise angle	V	Forward Speed
$C_{L\beta}$	Lift Coefficient for beta deadrise angle	VCG	Vertical Center of Gravity
CFD	Computational Fluid Dynamics	VP	Velocity profile
CoG	Center of Gravity	z_0	Vert. distance between CoG and calm water
F^R	Restoring forces in heave & pitch directions	$z(t)$	Effective vertical distance of the COG
F^{FL}	Flap forces in heave & pitch directions	Δ	Displacement
Fr	Length Froude Number	β	Deadrise angle
Fr_B	Beam Froude Number	$\tau(t)$	Effective trim angle
g	Gravitational acceleration	τ_0	Trim angle

GA	Genetic Algorithm	η_3	Heave motion
h	Blade height	η_5	Pitch motion
k_{YY}	Gyration radius for pitch motion	η_{5REF}	Optimum effective trim angle
L	Length Overall	$\lambda(t)$	Aspect ratio
L_F	Equivalent flap chord length	ρ	Water density
LCG	Longitudinal Center of Gravity	$\delta(t)$	Flap angle
l_P	Center of Pressure	σ	Flap span-beam ratio

Submitted: 09.09.2022. Omer Sinan Sahin, osinan.sahin@erdogan.edu.tr
Faculty of Maritime, Recep Tayyip Erdogan University

Accepted: 05.12.2022. Emre Kahramanoglu
Faculty of Naval Architecture and Maritime, Izmir Katip Celebi University
Ferdı Cakici
Naval Architecture and Maritime Faculty, Yildiz Technical University
Emre Pesman
Faculty of Marine Sciences, Karadeniz Technical University